

Diffusion-based Unsupervised Audio-visual Speech Enhancement

Jean-Eudes Ayilo¹, Mostafa Sadeghi¹, Romain Serizel¹, Xavier Alameda-Pineda²

¹Université de Lorraine, CNRS, Inria, Loria, Nancy, France

²Université Grenoble Alpes, Inria, Grenoble, France

jean-eudes.ayilo@inria.fr, mostafa.sadeghi@inria.fr, romain.serizel@loria.fr, xavier.alameda-pineda@inria.fr

Abstract—This paper proposes a new unsupervised audio-visual speech enhancement (AVSE) approach that combines a diffusion-based audio-visual speech generative model with a non-negative matrix factorization (NMF) noise model. First, the diffusion model is pre-trained on clean speech conditioned on corresponding video data to simulate the speech generative distribution. This pre-trained model is then paired with the NMF-based noise model to iteratively estimate clean speech. Specifically, a diffusion-based posterior sampling approach is implemented within the reverse diffusion process, where after each iteration, a speech estimate is obtained and used to update the noise parameters. Experimental results confirm that the proposed AVSE approach not only outperforms its audio-only counterpart but also generalizes better than a recent supervised-generative AVSE method. Additionally, the new inference algorithm offers a better balance between inference speed and performance compared to the previous diffusion-based method.

Index Terms—Unsupervised learning, audio-visual speech enhancement, diffusion models, posterior sampling.

I. INTRODUCTION

Speech enhancement (SE) refers to the problem of extracting a clean speech signal from a noisy recording. Early algorithms implemented for solving this task relied solely on acoustic features. However, speech production is inherently multimodal, involving movements of the lips and tongue, for example. Research in speech perception has demonstrated a crucial impact of visual cues on the ability of humans to focus their auditory attention on a speech signal [1]–[3]. Consequently, audio-visual speech enhancement (AVSE) has emerged as a new research trend. In this approach, lip movements are primarily used as complementary information to acoustic features to improve the performance, particularly in low signal-to-noise ratio (SNR) environments [1], [4].

Existing deep neural network (DNN)-based AVSE frameworks (and SE in general) are primarily divided into two learning approaches: supervised [5]–[12] and unsupervised [13]–[15]. Supervised methods, whether predictive or generative, involve training a DNN on pairs of clean and noisy speech, and possibly corresponding visual data. Specifically, predictive methods focus on mapping noisy speech directly to clean speech or to a time-frequency mask. In contrast, generative methods aim to generate clean speech at inference by learning the distribution of clean speech conditioned on the noisy input, rather than directly mapping from noisy to clean speech.

This work was supported by the French National Research Agency (ANR) under the project REAVISE (ANR-22-CE23-0026-01).

Some recent supervised-generative methodologies for SE [11], [16]–[19] leverage diffusion models [20]. A diffusion model learns data distribution by first pushing the clean data distribution towards a prior Gaussian distribution via the progressive corruption of the clean data with Gaussian noise. A DNN is trained to progressively transform samples drawn from the prior Gaussian distribution into clean data. In the diffusion-based supervised-generative SE context, the diffusion model which aims to learn clean speech distribution is conditioned on noisy speech. Lips video features can also be incorporated in such SE models as shown by [9]. As diffusion model inference requires many iterations, a faster alternative to [9], called FlowAVSE, was proposed in [10]. It is a two-stage method that uses in its first stage a supervised-predictive network that outputs an estimate of clean speech given the noisy speech and the lips video. Then, a conditional generative flow matching algorithm generates the final enhanced speech in just one sampling step, conditionally to the lips video and the output of the first stage. Despite their generative nature, these methods still require pairs of clean and noisy speech for training. Although all these supervised methods can generalize to unseen noise conditions at test time, a significant amount of paired data is needed [21], [22]. This is because it is impossible to train these models across all potential noise types and acoustic scenarios [13].

To enhance the robustness of SE models to unseen noises during training, some *unsupervised* methods have been developed that do not require a noise dataset. Here, the training stage involves learning the prior distribution of clean speech using models like variational auto-encoder (VAE) [14], [23] or dynamical VAE [15]. This learned prior is then combined with a noise model based on non-negative matrix factorization (NMF) [24] to estimate clean speech using expectation-maximization (EM). In this vein, Nortier *et al.* [25] recently introduced UDiffSE, an unsupervised audio-only SE framework utilizing diffusion models. In this approach, an unconditional diffusion model is trained on clean speech data. This diffusion model, serving as a prior for clean speech, is then combined with an NMF-based noise model to enhance speech. This method has been shown to outperform VAE-based SE approaches on some metrics and provides better generalization than its supervised counterpart, i.e., [11].

In this paper, we propose a diffusion-based AVSE framework that learns a clean speech distribution from audio-visual

(AV) data. The model incorporates visual features extracted from a self-supervised audio-visual speech representation learning model [26] as conditioning information. Additionally, we develop an iterative inference algorithm, named UDiffSE+, which operates significantly faster than UDiffSE. This approach substantially reduces the total number of iterations required, without dramatically degrading performance, as our experimental results will demonstrate.

II. DIFFUSION-BASED UNSUPERVISED SE

In this section, we review the diffusion-based unsupervised (audio-only) SE framework [25]. The modeling is done in the complex-valued short-time Fourier transform (STFT) domain. The observation model is $\mathbf{x} = \mathbf{s} + \mathbf{n}$, where \mathbf{x} , \mathbf{s} , and \mathbf{n} denote STFT arrays of noisy (mixture) speech, clean speech, and background noise, respectively. For notational simplicity, 2D STFT arrays (F frequency bins and T time frames) are represented by flattened 1D arrays, e.g., $\mathbf{s} \in \mathbb{C}^{FT}$.

A. Speech generative modeling

Learning a speech generative prior using diffusion models involves smoothly injecting noise into training samples, via a diffusion process $\{\mathbf{s}_t\}_{t \in [0,1]}$, which transforms clean training data $\mathbf{s}_0 = \mathbf{s}$ into Gaussian noise over time t . This can be described by the following *forward* stochastic differential equation (SDE) [20], [25]

$$d\mathbf{s}_t = \mathbf{f}(\mathbf{s}_t)dt + g(t)d\mathbf{w}, \quad (1)$$

where \mathbf{w} denotes a standard Wiener process, the vector-valued \mathbf{f} is the *drift* coefficient term, the scalar function g is the *diffusion* coefficient, and dt is an infinitesimal time-step. Here, $\mathbf{f}(\mathbf{s}_t) = -\gamma\mathbf{s}_t$, where γ is a constant parameter, and $g(t)$ controls the variance of the stochastic noise. The SDE in (1) has the *perturbation kernel* defined below, which allows one to directly sample \mathbf{s}_t given \mathbf{s}

$$p_{0t}(\mathbf{s}_t|\mathbf{s}) = \mathcal{N}_{\mathbb{C}}(\delta_t\mathbf{s}, \sigma(t)^2\mathbf{I}), \quad (2)$$

where $\delta_t = e^{-\gamma t}$, and the variance $\sigma(t)^2$ is determined from the SDE. Under some light regularity conditions [27], the noising process can be reverted through a *reverse* SDE:

$$d\mathbf{s}_t = [-\mathbf{f}(\mathbf{s}_t) + g(t)^2\nabla_{\mathbf{s}_t} \log p_t(\mathbf{s}_t)]dt + g(t)d\bar{\mathbf{w}}, \quad (3)$$

where $\bar{\mathbf{w}}$ is a standard Wiener process running backward in time. The term $\nabla_{\mathbf{s}_t} \log p_t(\mathbf{s}_t)$, known as the *score function*, is intractable to compute directly. It is thus approximated by a time-dependent DNN-based *score model*, denoted as $\mathbf{S}_\theta(\mathbf{s}_t, t)$. To learn θ , the following problem is solved [28]:

$$\theta^* = \operatorname{argmin}_{\theta} \mathbb{E}_{t, \mathbf{s}, \zeta, \mathbf{s}_t|\mathbf{s}} \left[\|\sigma(t)\mathbf{S}_\theta(\mathbf{s}_t, t) + \zeta\|_2^2 \right], \quad (4)$$

where $\zeta \sim \mathcal{N}_{\mathbb{C}}(\mathbf{0}, \mathbf{I})$ is a zero-mean complex-valued Gaussian noise. The reverse SDE can then be numerically solved, e.g., using the Predictor-Corrector (PC) sampler [20], to sample from the data distribution.

B. Unsupervised speech enhancement

The additive noise is modeled as $\mathbf{n} \sim \mathcal{N}_{\mathbb{C}}(\mathbf{0}, \operatorname{diag}(\mathbf{v}_\phi))$, where $\mathbf{v}_\phi = \operatorname{vec}(\mathbf{W}\mathbf{H})$, with \mathbf{W} , \mathbf{H} being low-rank matrices with non-negative entries, and $\operatorname{vec}(\cdot)$ denoting the vectorization operator. Given the pre-trained speech prior with frozen parameters θ^* , an iterative EM method is performed to update ϕ , where the M-step writes:

$$\max_{\phi} \mathbb{E}_{p_\phi(\mathbf{s}|\mathbf{x})} \{\log p_\phi(\mathbf{x}|\mathbf{s})\}. \quad (5)$$

The above expectation is approximated using a Monte Carlo estimate, which involves sampling from the intractable posterior $p_\phi(\mathbf{s}|\mathbf{x}) \propto p_\phi(\mathbf{x}|\mathbf{s})p(\mathbf{s})$ during the E-step. This approximation is implemented by substituting $\nabla_{\mathbf{s}_t} \log p_t(\mathbf{s}_t)$ in (3) with the following posterior-based score function:

$$\nabla_{\mathbf{s}_t} \log p_\phi(\mathbf{s}_t|\mathbf{x}) = \nabla_{\mathbf{s}_t} \log p_\phi(\mathbf{x}|\mathbf{s}_t) + \nabla_{\mathbf{s}_t} \log p_t(\mathbf{s}_t), \quad (6)$$

where the time-dependent likelihood $p_\phi(\mathbf{x}|\mathbf{s}_t)$ is approximated with a noise-perturbed pseudo-likelihood [25] and the score function is replaced with $\mathbf{S}_{\theta^*}(\mathbf{s}_t, t)$. Plugging the obtained clean speech estimate in (5), \mathbf{W} , \mathbf{H} are learned with multiplicative update rules. The EM steps are iteratively performed until convergence, typically requiring around five EM iterations for sufficient performance [25].

III. DIFFUSION-BASED UNSUPERVISED AVSE

This section presents our proposed unsupervised AVSE framework using diffusion models. We first develop an audio-visual speech prior model. Then, we propose a fast inference algorithm to estimate the clean speech.

A. Audio-visual speech generative model

We model the conditional speech generative distribution $p(\mathbf{s}|\mathbf{v})$, where \mathbf{v} denotes a visual embedding associated with \mathbf{s} . Following the diffusion-based framework discussed in Section II-A, a conditional score network $\mathbf{S}_\theta(\mathbf{s}_t, \mathbf{v}, t)$ is learned over clean AV speech data. The visual data denoted as $\mathbf{v} \in \mathbb{R}^{T_v \times p}$, where T_v represents the number of video frames and p indicates the embedding dimension, is incorporated into the score network as illustrated in Fig. 1.

To integrate audio and visual features within the score network, a cross-attention mechanism is employed at each downsampling and upsampling stage of the U-Net-like architecture. Here, audio features serve as queries, while visual features are used as keys and values. More specifically, we denote the acoustic embedding features at the i^{th} layer of the score network as $e_{a,i} \in \mathbb{R}^{C_i \times F_i \times T_i}$, where C_i represents the number of channels, and F_i and T_i indicate the embedding dimensions. Initially, the audio and visual features are projected into d_i -dimensional spaces for queries, keys, and values. This is followed by the computation of dot-product attention to produce a feature map of dimensions $C_i \times d_i \times T_i$. This feature map is then projected into an F_i -dimensional space, resulting in an intermediate audio-visual representation, $\tilde{e}_{av,i} \in \mathbb{R}^{C_i \times F_i \times T_i}$. The final audio-visual representation at layer i , denoted $e_{av,i}$, is achieved by adding the original

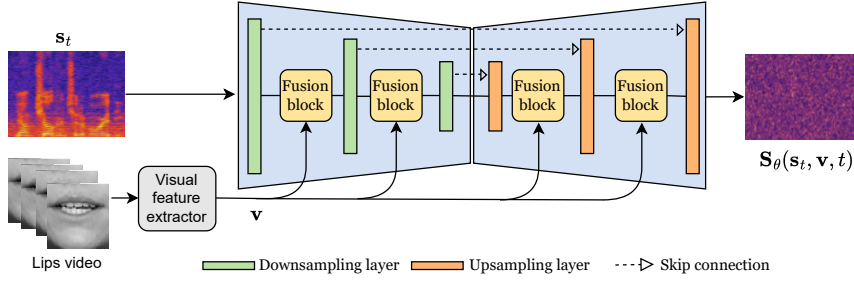


Fig. 1: Schematic diagram of the proposed AV-U-Net (score model) architecture.

acoustic embedding $e_{a,i}$ to the Group Normalized intermediate representation: $e_{av,i} = e_{a,i} + \text{GroupNorm}(\tilde{e}_{av,i})$.

B. Fast inference algorithm

The UDiffSE framework requires multiple rounds of an iterative reverse diffusion process as the E-step to obtain an estimation of the clean speech by sampling from the posterior $p_\phi(\mathbf{s}|\mathbf{x})$. This method is computationally intensive. We introduce a significantly more efficient methodology named UDiffSE+, which requires only one round of reverse diffusion.

This new framework leverages a clean speech estimate at each iteration of the reverse diffusion process, thereby eliminating the need for a complete reverse cycle. In this methodology, the noise parameters, *i.e.*, \mathbf{W} and \mathbf{H} , are updated following each reverse iteration based on the clean speech estimate obtained. This approach effectively employs an alternating maximization strategy, aimed at solving

$$\max_{\phi, \mathbf{s}} \log p_\phi(\mathbf{x}|\mathbf{s}) + \log p(\mathbf{s}), \quad (7)$$

by performing the following iterations

$$\begin{cases} \mathbf{s}_{0,k+1} = \underset{\mathbf{s}}{\operatorname{argmax}} \log p_{\phi_k}(\mathbf{x}|\mathbf{s}) + \log p(\mathbf{s}), & (8a) \\ \phi_{k+1} = \underset{\phi}{\operatorname{argmax}} \log p_\phi(\mathbf{x}|\mathbf{s}_{0,k+1}). & (8b) \end{cases}$$

Problem (8a), which is maximum a posteriori (MAP) estimation, can be solved by performing one reverse iteration, as done in UDiffSE, in which case, the iteration index k is replaced with a time discretization, denoted τ . To obtain an estimate of \mathbf{s} at iteration τ of the reverse diffusion process, denoted $\hat{\mathbf{s}}_{0,\tau}$, we leverage Tweedie's formula [29], that is

$$\hat{\mathbf{s}}_{0,\tau} = \mathbb{E}_{p_{\tau_0}(\mathbf{s}_0|\mathbf{s}_\tau)}[\mathbf{s}_0] \approx \frac{\mathbf{s}_\tau + \sigma_\tau^2 \mathbf{S}_{\theta^*}(\mathbf{s}_\tau, \tau)}{\delta_\tau}. \quad (9)$$

Plugging this into (8b), the parameters are updated by a single multiplicative update iteration. The overall (audio-only/AV) UDiffSE+ algorithm is described in Algorithm 1. By excluding lines 12 and 13, the algorithm simplifies to the E-step of UDiffSE. The highlighted box corresponds to the operations that ensure observation (\mathbf{x}) consistency, without which the algorithm reduces to prior sampling.

Algorithm 1 AV-UDiffSE+

Require: $\mathbf{x}, \mathbf{v}, N, \lambda, r$ (signal-to-noise ratio)

```

1:  $\mathbf{s}_1 \sim \mathcal{N}_{\mathcal{C}}(\mathbf{x}, \mathbf{I}), \Delta\tau \leftarrow \frac{1}{N}$ 
2: for  $i = N, \dots, 1$  do
3:    $\tau \leftarrow \frac{i}{N}$ 
4:    $\epsilon_\tau \leftarrow (\sigma_\tau \cdot r)^2$ 
5:    $\zeta_c \sim \mathcal{N}_{\mathcal{C}}(\mathbf{0}, \mathbf{I})$  ▷ (Corrector)
6:    $\mathbf{s}_\tau \leftarrow \mathbf{s}_\tau + \epsilon_\tau \mathbf{S}_{\theta^*}(\mathbf{s}_\tau, \mathbf{v}, \tau) + \sqrt{2\epsilon_\tau} \zeta_c$ 
7:    $\zeta_p \sim \mathcal{N}_{\mathcal{C}}(\mathbf{0}, \mathbf{I})$  ▷ (Predictor)
8:    $\mathbf{s}_\tau \leftarrow \mathbf{s}_\tau - \mathbf{f}_\tau \Delta\tau + g_\tau^2 \mathbf{S}_{\theta^*}(\mathbf{s}_\tau, \mathbf{v}, \tau) \Delta\tau + g_\tau \sqrt{\Delta\tau} \zeta_p$ 
9:   if  $i \equiv 0 \pmod{2}$  then ▷ (Posterior)
10:     $\nabla_{\mathbf{s}_\tau} \log \tilde{p}_\phi(\mathbf{x}|\mathbf{s}_\tau) \leftarrow \frac{1}{\delta_\tau} \left[ \frac{\sigma_\tau^2}{\delta_\tau^2} \mathbf{I} + \operatorname{diag}(\mathbf{v}_\phi) \right]^{-1} (\mathbf{x} - \frac{\mathbf{s}_\tau}{\delta_\tau})$ 
11:     $\mathbf{s}_\tau \leftarrow \mathbf{s}_\tau + \lambda g_\tau^2 \nabla_{\mathbf{s}_\tau} \log \tilde{p}_\phi(\mathbf{x}|\mathbf{s}_\tau) \Delta\tau$ 
12:     $\hat{\mathbf{s}}_{0,\tau} = \delta_\tau^{-1} (\mathbf{s}_\tau + \sigma_\tau^2 \mathbf{S}_{\theta^*}(\mathbf{s}_\tau, \mathbf{v}, \tau))$  ▷ (Estimate of  $\mathbf{s}_0$ )
13:     $\phi \leftarrow \operatorname{argmax}_\phi \log p_\phi(\mathbf{x}|\hat{\mathbf{s}}_{0,\tau})$  ▷ (Parameters update)
14:   end if
15: end for
16: return  $\hat{\mathbf{s}} = \mathbf{s}_0$ 

```

IV. EXPERIMENTS

Baselines. We compare the performance of our proposed method against two frameworks: the audio-only UDiffSE [25] and the supervised-generative FlowAVSE model [10].

Dataset. The TCD-TIMIT corpus [30] was employed for training. It comprises AV speech data from 56 English-speaking individuals with Irish accents, distributed among 39 for training, 8 for validation, and 9 for testing. The dataset features 98 distinct sentences, each approximately 5 seconds in duration and sampled at 16 kHz, totaling around 8 hours of data. Additionally, each spoken utterance is accompanied by a corresponding video, recording the speaker from a frontal perspective at a frame rate of 30 fps. We downsampled the videos to 25 fps and the lip regions of interest are extracted as 88×88 grayscale following [31], [32]. Training the supervised baseline model requires noisy speech counterparts. As such, we consider mixing TCD-TIMIT clean speech with DKITCHEN, OMEETING, PRESTO, PSTATION, NPARK noises from the DEMAND dataset [33] at $\{-10, 0, 10\}$ dB.

To evaluate SE performance, we define two scenarios: *matched* and *mismatched*, based on the origin of the test clean speech signals or noises. In the matched scenario, noisy speech is constructed by mixing clean speech from the TCD-TIMIT test set with noises from the DEMAND dataset (TMETRO, OOFFICE, TBUS, STRAFFIC, SPSQUARE). For each type of noise and SNR level, we randomly selected 10 utterances

TABLE I: Speech enhancement results in matched (TCD speech + DEMAND noise) and mismatched (LRS3 speech + NTCD noise) conditions. AO and AV denote audio-only and audio-visual models, respectively. EM represents the number of EM iterations, while RTF, the real-time factor, measures the average time needed to process one second of speech.

| Method | # Params (M) | EM | RTF ↓ | TCD speech + DEMAND noise | | | LRS3 speech + NTCD noise | | |
|---------------|--------------|----|-------------|---------------------------|-------------------|-------------------|--------------------------|-------------------|-------------------|
| | | | | SI-SDR ↑ | PESQ ↑ | ESTOI↑ | SI-SDR ↑ | PESQ ↑ | ESTOI↑ |
| Input | | | | 0.00 ±0.17 | 2.83 ±0.02 | 0.70 ±0.01 | 0.03 ±0.14 | 2.10 ±0.02 | 0.58 ±0.01 |
| UDiffSE [25] | 27.7 | 5 | 10.53 | 11.69 ±0.27 | 3.08 ±0.02 | 0.77 ±0.01 | 4.72 ±0.16 | 2.38 ±0.02 | 0.62 ±0.01 |
| FlowAVSE [10] | 60.2 | | 0.03 | 17.83 ±0.18 | 3.18 ±0.02 | 0.82 ±0.00 | 3.12 ±0.23 | 1.49 ±0.02 | 0.53 ±0.01 |
| AV-UDiffSE | 29.4 | 5 | 13.92 | 13.70 ±0.23 | 3.18 ±0.02 | 0.79 ±0.01 | 5.60 ±0.15 | 2.48 ±0.02 | 0.64 ±0.01 |
| AO-UDiffSE+ | 27.7 | 1 | 1.98 | 8.99 ±0.21 | 3.19 ±0.02 | 0.72 ±0.01 | 2.95 ±0.15 | 2.31 ±0.02 | 0.59 ±0.01 |
| AV-UDiffSE+ | 29.4 | 1 | 2.68 | 10.21 ±0.15 | 3.26 ±0.02 | 0.74 ±0.00 | 3.67±0.13 | 2.42 ±0.02 | 0.61 ±0.01 |

from each test speaker, totaling 900 evaluation utterances. In the mismatched scenario, we use the test set from the LRS3 dataset [34], consisting of 1321 clean speech files. These files are mixed randomly with one of the noise types from the NTCD-TIMIT dataset (Living Room, White, Car, Babble, Cafe) [35]. For both scenarios, the SNR levels are $\{-5, 5\}$ dB.

Evaluation metrics. We use standard SE metrics: the scale-invariant signal-to-distortion ratio (SI-SDR) in dB [36], the extended short-term objective intelligibility (ESTOI) measure [37], varying between $[0, 1]$, and the perceptual evaluation of speech quality (PESQ) score [38], with a range of $[-0.5, 4.5]$. For these metrics, higher values indicate better performance.

Model architecture. The base architecture in this paper, NCSN++M, is a lighter U-Net-like version of the original NCSN++ network [11]. In its audio-only configuration, NCSN++M comprises 27.8 million parameters. Integration of video data through cross-attention modules, each featuring a single attention head as detailed in Subsection III-A, results in a 6.13% increase in the total number of parameters. Additionally, the FlowAVSE baseline employs the NCSN++M network in both stages, totaling 60.2 million parameters. All in all, we trained from scratch the score networks for the audio-only and AV settings and the FlowAVSE networks.

Pretrained visual features. Similar to prior works [9], [39], [40], we extracted features from lip videos using the AV-HuBERT model [26], specifically utilizing its version fine-tuned for visual speech recognition. We maintained this visual encoder in a frozen state throughout our experiments. It processes silent grayscale videos and outputs visual features \mathbf{v} of size (T_v, p) , with $p = 768$, derived from the model’s final layer. For visual feature extraction in the FlowAVSE baseline, we followed the procedures outlined in the original paper [10].

Hyperparameters setting. We trained the diffusion models over 200 epochs using the Adam optimizer at a learning rate of 0.0001. For the STFT, a Hann window of 510 length and a hop length of 128 were used, yielding 256 frequency bins. Each speech waveform was randomly trimmed to 2.04 seconds, corresponding to $T = 256$ STFT time frames, to standardize input sizes for batching. The hyperparameters for the SDE and inference algorithm were aligned with those in [25].

Results. Table I presents the SE performance metrics for audio-only (AO) and audio-visual (AV) algorithms under

different conditions. In the matched scenario, the supervised baseline generally outperforms the unsupervised models in all metrics, except for AV-UDiffSE+ in PESQ, which aligns with the typical strengths of supervised methods in matched settings. Conversely, in the mismatched scenario, all methods, including the audio-only unsupervised models, surpass the FlowAVSE baseline by at least 0.55 dB in SI-SDR, 0.82 in PESQ, and 0.06 in ESTOI, except for AO-UDiffSE+ in SI-SDR. This indicates a potential for generalization in diffusion-based unsupervised SE frameworks, as also suggested by [25]. It is important to highlight that like supervised methods, unsupervised models also offer the flexibility to incorporate the visual modality. As expected, incorporating lip movements into the prior diffusion models (AV-UDiffSE+, AV-UDiffSE) enhances noise removal, speech quality, and intelligibility. For listening examples, please visit our project page¹.

We assessed the inference speed of various algorithms on an Nvidia A100-SXM4 (40GB), maintaining consistent conditions across all tests. Comparisons between UDiffSE and our proposed UDiffSE+ frameworks (in both audio-only and AV settings) revealed that UDiffSE, while superior in performance, requires significantly more processing time, as indicated by the real-time factor (RTF); it is approximately 5 times slower than UDiffSE+. Thus, UDiffSE+ offers a favorable compromise between inference speed and performance.

V. CONCLUSION

In this paper, we present a diffusion-based, unsupervised audio-visual speech enhancement (AVSE) framework, which leverages a diffusion model to simulate clean speech distribution, conditioned on visual cues from lip movements. The pre-trained diffusion model is integrated with an NMF-based noise model through an iterative process of reverse diffusion steps to estimate speech. Our experiments show that the proposed AVSE framework consistently outperforms its audio-only counterpart and offers better generalization than a recent supervised-generative approach [10]. Moreover, compared to the previous inference method [25], our algorithm achieves a better trade-off between performance and runtime. Future work includes a comprehensive subjective performance assessment.

¹https://jeaneudesayilo.github.io/fast_UDiffSE

REFERENCES

- [1] D. Michelsanti, Z.-H. Tan, S.-X. Zhang, Y. Xu, M. Yu, D. Yu, and J. Jensen, "An overview of deep-learning-based audio-visual speech enhancement and separation," *IEEE/ACM Transactions on Audio, Speech, and Language Processing*, vol. 29, pp. 1368–1396, 2021.
- [2] H. McGurk and J. MacDonald, "Hearing lips and seeing voices," *Nature*, vol. 264, no. 5588, pp. 746–748, 1976.
- [3] W. H. Sumby and I. Pollack, "Visual contribution to speech intelligibility in noise," *The journal of the acoustical society of america*, vol. 26, no. 2, pp. 212–215, 1954.
- [4] A. L. A. Blanco, C. Valentini-Botinhao, O. Klejch, M. Gogate, K. Dashtipour, A. Hussain, and P. Bell, "AVSE challenge: Audio-visual speech enhancement challenge," in *IEEE Spoken Language Technology Workshop (SLT)*, 2023, pp. 465–471.
- [5] T. Alfouras, J. Chung, and A. Zisserman, "The conversation: Deep audio-visual speech enhancement," in *Interspeech*, 2018.
- [6] J.-C. Hou, S.-S. Wang, Y.-H. Lai, Y. Tsao, H.-W. Chang, and H.-M. Wang, "Audio-visual speech enhancement using multimodal deep convolutional neural networks," *IEEE Transactions on Emerging Topics in Computational Intelligence*, vol. 2, no. 2, pp. 117–128, 2018.
- [7] S.-Y. Chuang, H.-M. Wang, and Y. Tsao, "Improved lite audio-visual speech enhancement," *IEEE/ACM Transactions on Audio, Speech, and Language Processing*, vol. 30, pp. 1345–1359, 2022.
- [8] T. Afouras, J. S. Chung, and A. Zisserman, "My lips are concealed: Audio-visual speech enhancement through obstructions," in *Interspeech*, 2019.
- [9] J. Richter, S. Frintrop, and T. Gerkmann, "Audio-visual speech enhancement with score-based generative models," in *Proc. ITG Conf. Speech Communication*, 2023.
- [10] C. Jung, S. Lee, J.-H. Kim, and J. S. Chung, "FlowAVSE: Efficient audio-visual speech enhancement with conditional flow matching," in *Proc. INTERSPEECH*, 2024, pp. 2210–2214.
- [11] J. Richter, S. Welker, J.-M. Lemerrier, B. Lay, and T. Gerkmann, "Speech enhancement and dereverberation with diffusion-based generative models," *IEEE/ACM Transactions on Audio, Speech, and Language Processing*, 2023.
- [12] S. Pascual, A. Bonafonte, and J. Serrà, "Segan: Speech enhancement generative adversarial network," *Interspeech 2017*, p. 3642, 2017.
- [13] X. Bie, S. Leglaive, X. Alameda-Pineda, and L. Girin, "Unsupervised speech enhancement using dynamical variational autoencoders," *IEEE/ACM Transactions on Audio, Speech, and Language Processing*, vol. 30, pp. 2993–3007, 2022.
- [14] M. Sadeghi, S. Leglaive, X. Alameda-Pineda, L. Girin, and R. Horaud, "Audio-visual speech enhancement using conditional variational autoencoders," *IEEE/ACM Transactions on Audio, Speech, and Language Processing*, vol. 28, pp. 1788–1800, 2020.
- [15] A. Golmakani, M. Sadeghi, and R. Serizel, "Audio-visual speech enhancement with a deep Kalman filter generative model," in *IEEE International Conference on Acoustics, Speech and Signal Processing (ICASSP)*, 2023, pp. 1–5.
- [16] P. Gonzalez, Z.-H. Tan, J. Østergaard, J. Jensen, T. S. Alstrøm, and T. May, "Diffusion-based speech enhancement in matched and mismatched conditions using a heun-based sampler," in *ICASSP 2024-2024 IEEE International Conference on Acoustics, Speech and Signal Processing (ICASSP)*. IEEE, 2024, pp. 10431–10435.
- [17] J. Serrà, S. Pascual, J. Pons, R. O. Araz, and D. Scaini, "Universal speech enhancement with score-based diffusion," *arXiv preprint arXiv:2206.03065*, 2022.
- [18] Y.-J. Lu, Z.-Q. Wang, S. Watanabe, A. Richard, C. Yu, and Y. Tsao, "Conditional diffusion probabilistic model for speech enhancement," in *IEEE International Conference on Acoustics, Speech and Signal Processing (ICASSP)*, 2022, pp. 7402–7406.
- [19] H. Yen, F. G. Germain, G. Wichern, and J. Le Roux, "Cold diffusion for speech enhancement," in *IEEE International Conference on Acoustics, Speech and Signal Processing (ICASSP)*, 2023, pp. 1–5.
- [20] Y. Song, J. Sohl-Dickstein, D. P. Kingma, A. Kumar, S. Ermon, and B. Poole, "Score-based generative modeling through stochastic differential equations," in *International Conference on Learning Representations (ICLR)*, 2021.
- [21] X. Lin, S. Leglaive, L. Girin, and X. Alameda-Pineda, "Unsupervised speech enhancement with deep dynamical generative speech and noise models," *arXiv preprint arXiv:2306.07820*, 2023.
- [22] P. Gonzalez, Z.-H. Tan, J. Østergaard, J. Jensen, T. S. Alstrøm, and T. May, "The effect of training dataset size on discriminative and diffusion-based speech enhancement systems," *arXiv preprint arXiv:2406.06160*, 2024.
- [23] G. Carbajal, J. Richter, and T. Gerkmann, "Disentanglement learning for variational autoencoders applied to audio-visual speech enhancement," in *2021 IEEE Workshop on Applications of Signal Processing to Audio and Acoustics (WASPAA)*. IEEE, 2021, pp. 126–130.
- [24] D. Lee and H. S. Seung, "Algorithms for non-negative matrix factorization," *Advances in neural information processing systems*, vol. 13, 2000.
- [25] B. Nortier, M. Sadeghi, and R. Serizel, "Unsupervised speech enhancement with diffusion-based generative models," in *IEEE International Conference on Acoustics, Speech and Signal Processing (ICASSP)*, 2024.
- [26] B. Shi, W.-N. Hsu, K. Lakhota, and A. Mohamed, "Learning audio-visual speech representation by masked multimodal cluster prediction," *arXiv preprint arXiv:2201.02184*, 2022.
- [27] B. D. Anderson, "Reverse-time diffusion equation models," *Stochastic Processes and their Applications*, vol. 12, no. 3, pp. 313–326, 1982.
- [28] D. P. Kingma and R. Gao, "Understanding diffusion objectives as the elbo with simple data augmentation," in *Thirty-seventh Conference on Neural Information Processing Systems*, 2023.
- [29] B. Efron, "Tweedie's formula and selection bias," *Journal of the American Statistical Association*, vol. 106, no. 496, pp. 1602–1614, 2011.
- [30] N. Harte and E. Gillen, "TCD-TIMIT: An audio-visual corpus of continuous speech," *IEEE Transactions on Multimedia*, vol. 17, no. 5, pp. 603–615, 2015.
- [31] P. Ma, S. Petridis, and M. Pantic, "Visual speech recognition for multiple languages in the wild," *Nature Machine Intelligence*, vol. 4, no. 11, pp. 930–939, 2022.
- [32] Y. Yemini, A. Shamsian, L. Bracha, S. Gannot, and E. Fetaya, "Lipvoicer: Generating speech from silent videos guided by lip reading," in *The Twelfth International Conference on Learning Representations*, 2024.
- [33] J. Thiemann, N. Ito, and E. Vincent, "The diverse environments multichannel acoustic noise database (DEMAND): A database of multichannel environmental noise recordings," in *Proceedings of Meetings on Acoustics*. AIP Publishing, 2013, vol. 19.
- [34] T. Afouras, J. S. Chung, and A. Zisserman, "Lrs3-ted: a large-scale dataset for visual speech recognition," *ArXiv*, vol. abs/1809.00496, 2018.
- [35] A. H. Abdelaziz et al., "NTCD-TIMIT: A new database and baseline for noise-robust audio-visual speech recognition," in *Interspeech*, 2017, pp. 3752–3756.
- [36] J. Le Roux, S. Wisdom, H. Erdogan, and J. R. Hershey, "SDR—half-baked or well done?," in *IEEE International Conference on Acoustics, Speech and Signal Processing (ICASSP)*, 2019.
- [37] J. Jensen and C. H. Taal, "An algorithm for predicting the intelligibility of speech masked by modulated noise maskers," *IEEE/ACM Transactions on Audio, Speech, and Language Processing*, vol. 24, no. 11, pp. 2009–2022, 2016.
- [38] A. W. Rix, J. G. Beerends, M. P. Hollier, and A. P. Hekstra, "Perceptual evaluation of speech quality (PESQ)—a new method for speech quality assessment of telephone networks and codecs," in *IEEE international conference on acoustics, speech, and signal processing. Proceedings (ICASSP)*, 2001, vol. 2, pp. 749–752.
- [39] I.-C. Chern, K.-H. Hung, Y.-T. Chen, T. Hussain, M. Gogate, A. Hussain, Y. Tsao, and J.-C. Hou, "Audio-visual speech enhancement and separation by utilizing multi-modal self-supervised embeddings," in *2023 IEEE International Conference on Acoustics, Speech, and Signal Processing Workshops (ICASSPW)*. IEEE, 2023, pp. 1–5.
- [40] J.-C. Chou, C.-M. Chien, and K. Livescu, "Av2wav: Diffusion-based re-synthesis from continuous self-supervised features for audio-visual speech enhancement," in *ICASSP 2024-2024 IEEE International Conference on Acoustics, Speech and Signal Processing (ICASSP)*. IEEE, 2024, pp. 10806–10810.